Cancer Research

NR1D1 Recruitment to Sites of DNA Damage Inhibits Repair and Is Associated with Chemosensitivity of Breast Cancer

Na-Lee Ka[1], Tae-Young Na[1], Hyelin Na[1], Min-Ho Lee[1], Han-Su Park[1], Sewon Hwang[1], Il Yong Kim[2], Je Kyung Seong[2], and Mi-Ock Lee[1]

Abstract

DNA repair capacity is critical for survival of cancer cells upon therapeutic DNA damage and thus is an important determinant of susceptibility to chemotherapy in cancer patients. In this study, we identified a novel function of nuclear receptor NR1D1 in DNA repair, which enhanced chemosensitivity in breast cancer cells. NR1D1 inhibited both nonhomologous end joining and homologous recombination double-strand breaks repair, and delayed the clearance of γH2AX DNA repair foci that formed after treatment of doxorubicin. PARylation of NR1D1 by PARP1 drove its recruitment to damaged DNA lesions. Deletion of the ligand binding domain of NR1D1 that interacted with PARP1, or treatment of 6-(5H)-phenanthridinone, an inhibitor of PARP1, suppressed the recruitment of NR1D1 to DNA damaged sites, indicating PARylation as a critical step for the NR1D1 recruitment. NR1D1 inhibited recruitment of the components of DNA damage response complex such as SIRT6, pNBS1, and BRCA1 to DNA lesions. Downregulation of NR1D1 in MCF7 cells resulted in resistance to doxorubicin, both *in vitro* and *in vivo*. Analysis of four public patient data sets indicated that NR1D1 expression correlates positively with clinical outcome in breast cancer patients who received chemotherapy. Our findings suggest that NR1D1 and its ligands provide therapeutic options that could enhance the outcomes of chemotherapy in breast cancer patients. *Cancer Res; 77(9); 2453–63. ©2017 AACR.*

Introduction

Breast cancer is the most commonly diagnosed cancer in women and the fifth leading cause of cancer-related death worldwide (1). In general, the primary treatment for patients with breast cancer is surgery and subsequent adjuvant chemotherapy is treated to improve the survival of patients by eradicating residual cancer cells (2). Anthracyclines (e.g., doxorubicin and epirubicin), alkylating agents (e.g., cyclophosphamide), and taxanes (e.g., paclitaxel and doxetaxel) comprise the standard chemotherapy regimens for the treatment of breast cancer (3). In addition, platinum-based agents have been considered as a component of combination therapy, especially for the treatment of patients with triple-negative breast cancer (TNBC; ref. 4). However, despite their known efficacy, drug resistance develops frequently in breast cancer patients, which is still a major obstacle in the treatment of cancer. Therefore, there is an urgent need to develop new therapeutic strategies to enhance the effectiveness of chemotherapy while reducing the rate of resistance.

Most chemotherapeutic agents exert cytotoxic effects by inducing excessive DNA lesions. DNA double-strand breaks (DSB) are considered the most hazardous lesions that generated by ionizing radiation or topoisomerase II inhibitors such as etoposide and doxorubicin. DSBs are repaired by two major pathways; nonhomologous end joining (NHEJ) and homologous recombination (HR; ref. 5). In normal cells, multiple mechanisms have evolved to facilitate the rapid recognition of DNA lesions by DNA damage response (DDR) factors, which activate cell-cycle checkpoints and direct DNA repair (6). In contrast, many types of cancer cells possess specific defects in DDR pathways such as mutations in the breast cancer susceptibility gene (*BRCA*) and *p53*, which alter the sensitivity of the rapidly growing cancer cells to chemotherapy (7). However, some cancer cells develop the capacity to back-up DNA repair pathways such as genetic reversion of DDR defects or alterations of their choice of DNA repair pathway, which could induce resistance to chemotherapy in cancer cells (8). Thus, regulating the components of DNA repair networks is a critical factor that determines the response as well as resistance to chemotherapeutic drugs. Recent studies have identified several novel regulatory factors that confer sensitivity to chemo- or radiosensitivity by controlling DDR components in breast cancer cells. For example, tumor protein D52 increases the sensitivity to ionizing radiation-induced DNA damage by compromising ataxia telangiectasia mutated (ATM)-mediated DDR in breast cancer cells (9). FOXP3, an X-linked tumor suppressor gene, decreases HR-mediated DNA repair and sensitizes cancer cells to γ-irradiation by repressing the transcriptional expression of BRCA1 (10). These genes are overexpressed or mutated in many types of cancers; therefore, characterizing the gene expression signatures of these DDR defects in cancer cells may help to develop biomarkers that could predict therapeutic responses.

[1]College of Pharmacy and Bio-MAX Institute, Seoul National University, Gwanak-gu, Seoul, Korea. [2]College of Veterinary Medicine, Seoul National University and Korea Mouse Phenotyping Center, Gwanak-gu, Seoul, Korea.

Note: Supplementary data for this article are available at Cancer Research Online (http://cancerres.aacrjournals.org/).

Corresponding Author: Mi-Ock Lee, College of Pharmacy, Seoul National University, 1 Gwanak-ro, Gwanak-gu, Seoul 08826, Korea. Phone: 82-2-880-9331; Fax: 82-2-887-2692; E-mail: molee@snu.ac.kr

doi: 10.1158/0008-5472.CAN-16-2099

Nuclear receptor subfamily 1, group D, member 1 (NR1D1; Rev-erbα), an orphan nuclear receptor, functions as a circadian clock that participates in regulation of the circadian rhythm and metabolic homeostasis (11). Interestingly, the *NR1D1* gene is encoded within the *ERBB2* amplicon (17q12–q21), a marker of aggressive breast tumors, and the expression level of this receptor is correlated with a poor prognosis (12, 13). In agreement with these observations, NR1D1 enhances the survival of breast cancer cells by upregulating several genes in the *de novo* fatty acid synthase network associated with aerobic glycolysis (14). However, results of recent studies controversially showed that expression of NR1D1 was lower in both estrogen receptor (ER)-positive and ER-negative breast cancer cohorts compared with normal breast subjects (15). Furthermore, a synthetic NR1D1 and NR1D2 agonist, SR9011, suppressed the proliferation of breast cancer cells irrespective of their ER or ERBB2 status (16). These studies suggest a role for NR1D1 in breast cancer proliferation and cellular energy metabolism, but its roles in DNA repair and chemosensitivity are not known. In this study, therefore, we asked whether NR1D1 affected DNA repair after damage induced by a chemotherapeutic agent, doxorubicin, in breast cancer cells and further analyzed the correlation between the expression level of NR1D1 with the overall survival rate after chemotherapy in patients with breast cancer.

Materials and Methods

Cell culture and reagents

Human breast cancer cell lines, that is, MCF7, ZR75-1, BT474, MDA-MB-231, T47D, and SKBR3 were obtained from the ATCC. These cells were authenticated by ATCC, by short tandem repeat profiling and monitoring cell morphology. The DSB reporter cell line (U2OS) was provided by Dr. Janicki (The Wistar Institute, Philadelphia, PA). MCF7, ZR75-1, BT474, MDA-MB-231, and U2OS cells were maintained in DMEM supplemented with 10% FBS. T47D and SKBR3 cells were maintained in RPMI1640 medium supplemented with 10% FBS. The cells were grown in an incubator with 5% CO_2/95% air at 37°C. 5-bromo-2′-deoxyuridine, doxorubicin, 6-(5H)-phenanthridinone (PHEN), GSK4112, and 3-(4,5-dimethylthiazol-2-yl)-2,5-diphenyltetrazolium bromide (MTT) were purchased from Merck.

Plasmids and transient transfection

FLAG- or Myc-tagged deletion mutants of NR1D1, that is, N-terminus (NT; amino acids (aa), 1–130), DNA binding domain (DBD; aa 131–188), hinge (aa 189–286), ligand binding domain (LBD; aa 287–614), hinge with LBD (HinL; aa 189–614), ΔHinge (hinge deleted), and ΔLBD (aa 1–286) were constructed by inserting the corresponding cDNA into p3XFLAG-CMV-10 (Merck) or pCMV-Myc (Clontech; ref. 17). FLAG-tagged deletion mutants of PARP1, that is, DBD (aa 1–372), BRCA1 C-terminal domain (BRCT; aa 373–524), and catalytic domain (CatD; aa 525–1014), were constructed by inserting the corresponding cDNA into p3XFLAG-CMV-10. NHEJ and HR reporter plasmids, as well as the I-*Sce*I expression vector were kindly donated by Dr. Vera Gorbunova (University of Rochester, Rochester, NY; ref. 18). The wild-type and the mutant D450A FokI were kindly provided by Dr. Price (Dana-Farber Cancer Institute, Boston, MA; ref. 19). H2AX-GFP and GFP-RAP80 were provided by Dr. Hyeseong Cho (Ajou University, Suwon, South Korea) and Dr. Hongtae Kim (Sungkyunkwan University, Suwon, South Korea), respectively (20, 21). Transient transfection of plasmids was performed as described previously (22).

Analysis of DNA repair

To assess the DSB repair efficiency, cells were cotransfected with the *Hin*dIII-linearized NHEJ or I-*Sce*I-linearized HR reporter plasmid, Myc-NR1D1, and DsRed expression vector. The numbers of GFP-positive and DsRed-positive cells were determined by flow cytometry, and the ratio between GFP-positive and DsRed-positive cells was quantified as described previously (23). Laser microirradiation experiments were performed as described previously using a Zeiss LSM 710 confocal microscope (Carl Zeiss; ref. 24) and the fluorescence intensity was normalized against the initial intensity. FokI assay was performed as described previously (19). Recruitment of DNA repair factors to the damaged DNA sites was analyzed in a Chromatin immunoprecipitation (ChIP) assay using specific antibodies against Myc (#40), PARP1 (#1561), BRCA1 (#6954; Santa Cruz Biotechnology), phospho-p95/NBS1 (#3001), Sirt6 (#2590; Cell Signaling), or γH2AX (#ab22551; Abcam) as described previously (18, 24).

Western blotting, immunoprecipitation, qRT-PCR, immunofluorescence, and *in situ* proximity ligation assay

Western blotting and immunoprecipitation were performed as described previously using specific antibodies against NR1D1 (#14506-1-AP; Proteintech), PARP1 (#1561), Myc (#40; Santa Cruz Biotechnology), FLAG (#F3165; Merck), PAR (#551813; BD Biosciences), actin (#1616; Santa Cruz), or α-tubulin (#05-829; Calbiochem; ref. 22). qRT-PCR was performed using specific primers (Supplementary Table S1), as described previously (25). During immunofluorescence staining, cells were fixed and stained with the antibodies against NR1D1 (1:200; #14506-1-AP; Proteintech), γH2AX (1:100; #ab22551; Abcam), or p53-binding protein 1 (53BP1; 1:100; #ab36823; Abcam). To detect protein–protein interactions with high selectivity and sensitivity, proximity ligation assays (PLA) were performed using specific antibodies against NR1D1 (#14506-1-AP; Proteintech) and PARP1 (#1561; Santa Cruz), with the Duolink II Detection Reagent Red (#DUO92008; Merck), as described previously (24).

In vitro PARylation assay

For the *in vitro* PARylation assay, the recombinant GST–PARP1 protein (#SRP0192; Merck) was incubated with a reaction buffer containing 20 mmol/L Tris-HCl (pH 8.0), 100 mmol/L NaCl, 10 mmol/L $MgCl_2$, 10% glycerol, 1 mmol/L DTT, 0.1 mg/mL sonicated salmon sperm DNA, and 300 μM NAD^+, in the presence or absence of the recombinant GST–NR1D1–His for 30 min at 30°C. The reaction mixture was analyzed by Western blotting using anti-PAR antibody. The purified recombinant GST–NR1D1–His protein was obtained as described previously (24).

Establishment of stable cell lines and measurement of cell survival

The lentiviral vector encoding NR1D1 (pLJM1-NR1D1) or shNR1D1 (pLKO.1-shNR1D1) was constructed by inserting full-length NR1D1 or an annealed oligomer, respectively, into the *Age*I/*Eco*RI site of the corresponding viral vector (Supplementary Table S1). Production of the virus, transduction into MCF7

cells, and selection of stable clones were performed as described previously (22). The MTT assay was performed to quantify cell survival. Cells were seeded onto 96-well plates and treated with doxorubicin for 3 days. To assess the viability of cells in 3D cultures, 48-well plates were coated with Matrigel (BD Biosciences) and the cell suspension mixed with Matrigel was then seeded on top. Cells were incubated in medium containing doxorubicin and/or GSK4112. To assess the clonogenic survival ability, cells were seeded in 35-mm plates. After incubation for 48 hours, cells were treated with doxorubicin and/or GSK4112 for 14 days. At the end of the treatment, colonies were fixed with methanol, stained with 0.5% crystal violet, and the colonies (>50 cells) were counted.

Xenograft experiments and histologic analysis

Animal experiments were conducted in accordance with the guidelines of Seoul National University Institutional Animal Care and Use Committee. Female 6-week-old athymic (nu/nu) BALB/c mice (Central Lab. Animal Inc.) were housed in an air-conditioned room at a temperature of 22°C to 24°C and humidity of 37% to 64%, with a 12-hour light/dark cycle. Mice were implanted subcutaneously with 17β-estradiol pellets (60-day release; Innovative Research of America) and then injected in both flanks with 5×10^6 MCF-7 cells mixed 1:1 with Matrigel. When the tumor volume reached approximately 100 mm^3, mice were separated randomly into two groups and given intraperitoneal injections with saline or doxorubicin at a dose of 4 mg/kg at 4-day intervals, with a total of three injections. The tumor diameter was measured every 3 days with a caliper and the tumor volume was calculated using the following formula: tumor volume (mm^3) = $width^2 \times length \times 0.5$ (22). Immunohistochemistry was performed using γH2AX antibody (#ab22551; Abcam) as described previously (25).

For immunohistochemistry or PLA assays of breast cancer tissues, tissue microarray slides (#T088c, US Biomax) were deparaffinized and processed for antigen retrieval. Slides were subjected to immunostaining using antibodies against γH2AX (#ab22551; Abcam) and NR1D1 (#14506-1-AP; Proteintech).

Breast cancer patient cohort analysis based on public datasets

The public datasets, GSE4056, GSE34138, and GSE1456, were downloaded from NCBI Gene Expression Omnibus (GEO; http://www.ncbi.nlm.nih.gov/geo/) and the NKI dataset was obtained from a Web site provided by Dr. Bernards and his colleagues (http://ccb.nki.nl/data/). The GSE4056 dataset (DKFZ/Operon Human Oligo Set v2.1) contained the gene expression profiles of a 100-patient cohort, among which 44 patients in the validation set had received gemcitabine, epirubicin, and docetaxel as primary standard chemotherapy (26). The GSE34138 dataset (HumanWG-6 v3.0 Expression BeadChip; Illumina) contained the gene expression profiles of a 178-patient cohort treated with a single dose-dense doxorubicin and cyclophosphamide chemotherapy regimen (27). The GSE1456 dataset (Affymetrix Human Genome U133A Array) contained the gene expression profiles of a 159-patient cohort who had mostly been treated with intravenous cyclophosphamide, methotrexate, and 5-fluorouracil as adjuvant chemotherapy (28). The NKI dataset (Agilent chip containing NKI annotated probes) included the gene expression profiles of a 295-patient cohort, among which 110 patients who received chemotherapy were selected for analysis (29). Data that lacked expression signals in the microarrays or without clinical information records were excluded from all analyses. The processed data including normalization procedures were obtained from the corresponding websites and no additional transformations were performed.

Statistical analyses

Statistical analyses were performed using GraphPad Prism software. Experimental values were expressed as the mean ± SD based on three independent experiments, unless indicated otherwise. Statistically significant differences between two groups were determined using the nonparametric Mann–Whitney *U* test. Statistical analyses of multiple groups were performed using two-way ANOVA followed by the Bonferroni posttest. $P < 0.05$ was considered significantly different. Flow cytometry results, laser microirradiation data, immunofluorescence data, immunoblots, *in situ* PLAs, FokI assays, and clonogenic survival assays were taken from a representative experiment, which was qualitatively similar to at least three experiments.

Results

NR1D1 inhibits DNA repair in breast cancer cells

To assess the role of NR1D1 in DNA repair, first, we determined whether NR1D1 affected DNA repair after DSB using the plasmid-based NHEJ and HR repair reporter assays. We found that both HR and NHEJ efficiency were reduced by approximately 50% to 60% when NR1D1 was transiently overexpressed (Fig. 1A and Supplementary Fig. S1A). The mRNA level of NR1D1 and the NHEJ repair efficiency in several different types of breast cancer cell lines were negatively correlated, which might suggest that NR1D1 disrupts the correct DNA repair process in these cells (Fig. 1B). Thus, we asked whether NR1D1 could alter the rate of recruitment of DDR complex at DNA breakage sites by employing GFP-RAP80 and H2AX-GFP using laser microirradiation assay. The rate and intensity of GFP from the fusion proteins at damaged sites were significantly lower in the NR1D1-expressing cells compared with those in the control cells (Fig. 1C and Supplementary Fig. S1B and S2A). Next, we used doxorubicin, a DNA intercalating agent causing DSBs and subsequent DDR response, to monitor clearance of γH2AX foci (30). The number of γH2AX foci, an indicator of unrepaired DNA damage, increased greatly after doxorubicin treatment in MCF7 cells but it decreased with time after the removal of the drug. However, the γH2AX foci remained longer in the nucleus when NR1D1 was overexpressed, indicating a delayed γH2AX foci clearance by NR1D1 (Fig. 1D and Supplementary Fig. S1C). Similar results were obtained when 53BP1 foci clearance was examined (Supplementary Fig. S2B). Together these results show that DNA repair is impaired in the presence of NR1D1.

PARP1 interacts with NR1D1 and induces subsequent PARyation

Next, we asked the mechanism by which NR1D1 impairs DNA repair. Because PARP1 regulates the first step in DDR response by catalyzing the attachment of PAR chains to target proteins, which precede the γH2AX recruitment to DNA breakage sites, we examined the potential interaction of NR1D1 with PARP1 (31). Coimmunoprecipitation experiments showed that both endogenous and FLAG-tagged NR1D1 interacted with PARP1 and this interaction was enhanced in response to the

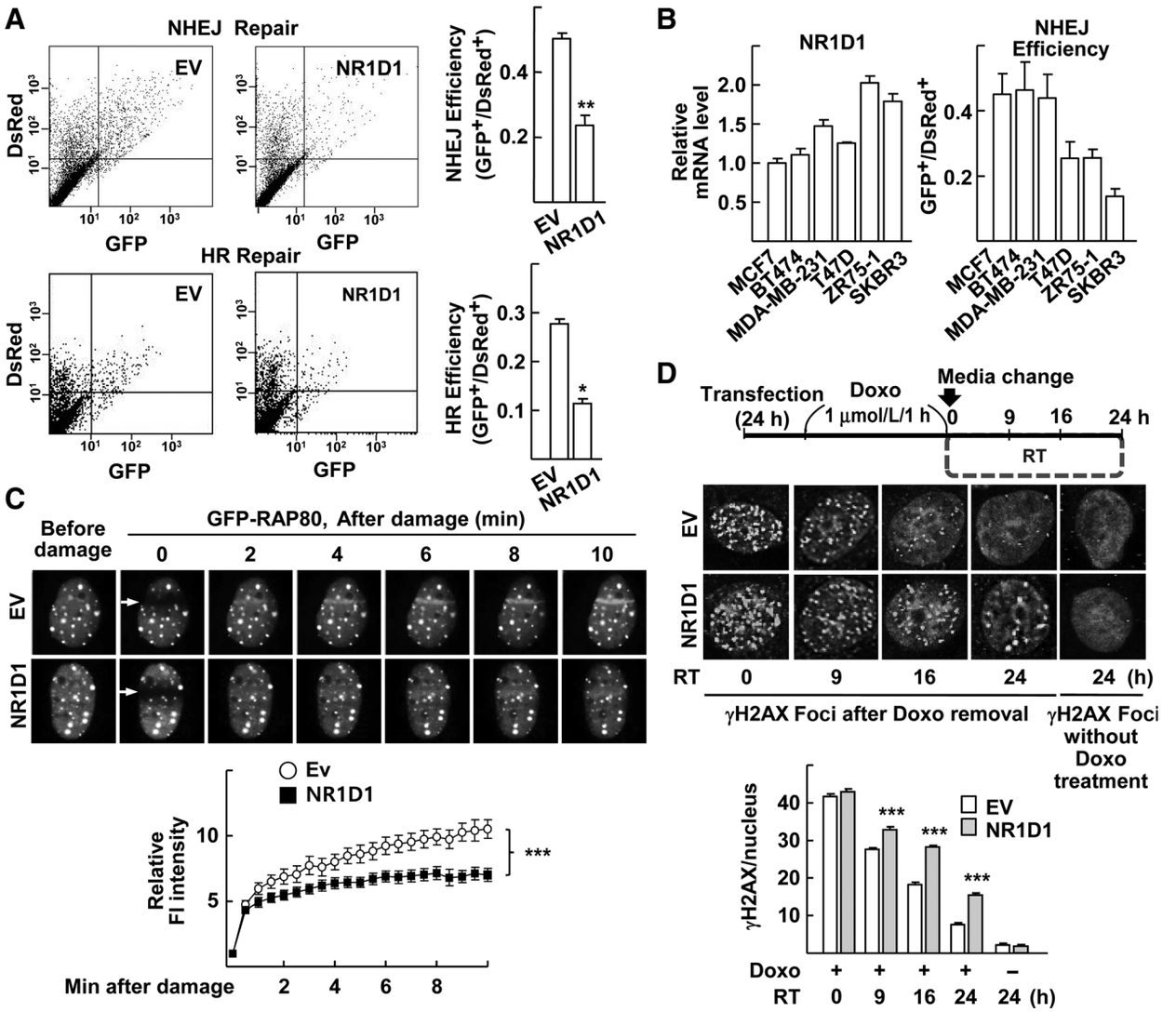

Figure 1.

NR1D1 inhibits DNA repair in various breast cancer cell lines. **A,** NHEJ or HR efficiency was measured in MCF7 cells that were cotransfected with the *Hin*dIII-linearized NHEJ or I-*Sce*I-linearized HR reporter plasmid, Ds-Red, and either empty vector (EV) or Myc-NR1D1. The ratio of number of GFP-positive cells versus that of DsRed-positive cells was determined by flow cytometry. *, $P < 0.05$; **, $P < 0.01$ versus EV ($n = 4$). Expression level of NR1D1 was shown as control in Supplementary Fig. S1A. **B,** Expression level of NR1D1 from indicated cells was analyzed by qRT-PCR (left; $n = 3$). NHEJ efficiency was measured as described in **A**. **C,** Laser microirradiation experiments were performed with MCF7 cells that stably expressed empty vector or Myc-NR1D1 after transfection of GFP-RAP80 and treatment of 5-bromo-2′-deoxyuridine (top). The mean fluorescence (FI) intensity at the microirradiated site was analyzed (bottom). The arrows indicate the site of irradiation. ***, $P < 0.001$. Expression level of NR1D1 was shown as control in Supplementary Fig. S1B. **D,** Clearance of γH2AX was monitored in MCF7 cells that were transfected with empty vector or FLAG-NR1D1 and were treated with 1 μmol/L doxorubicin (Doxo) for 1 hour. Cells were fixed at the indicated recovery time (RT) points after doxorubicin removal and were immunostained with anti-γH2AX antibody. Nuclei were visualized by DAPI staining (gray; top). The number of γH2AX foci was quantified from 50 cells (bottom). ***, $P < 0.001$ vs. empty vector at each time point ($n = 3$). Expression level of NR1D1 is shown as control in Supplementary Fig. S1C.

treatment of either doxorubicin or GSK4112, a ligand of NR1D1 (Fig. 2A and Supplementary Fig. S3A). *In situ* PLA further confirmed this physical interaction (Fig. 2B). Deletion mapping studies demonstrated that the LBD of NR1D1 and the DBD of PARP1 were responsible for this interaction (Supplementary Fig. S3B and S3C). Interestingly, NR1D1 was PARylated and the PARylation was stronger in the presence of doxorubicin in MCF7 cells (Fig. 2C). *In vitro* PARylation assay using recombinant NR1D1 and PARP1 proteins clearly confirmed the PARylation of NR1D1 (Fig. 2D). Domain mapping study showed that the hinge domain of NR1D1 was PARylated, and both the hinge domain deletion mutant (ΔHinge) and the LBD deletion mutant (ΔLBD) were not PARylated (Supplementary Fig. S3D and Fig. 2E). The ΔHinge and ΔLBD were less effective in inhibiting NHEJ and HR repair compared with the full-length NR1D1, indicating that the PARylation of NR1D1 is important in NR1D1-induced inhibition of DNA repair (Fig. 2F and Supplementary Fig. S1D).

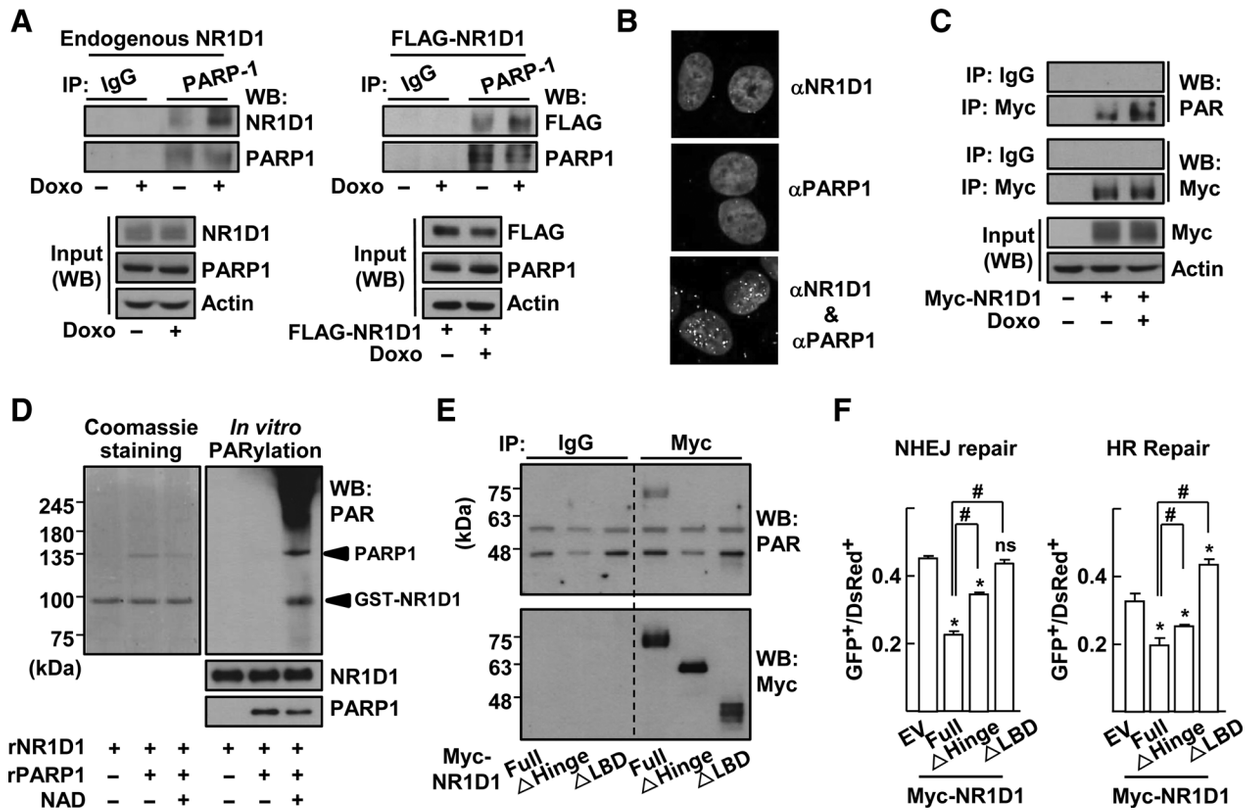

Figure 2.

NR1D1 binds PARP1 and it is PARylated in response to DNA damage. **A,** Coimmunoprecipitation of NR1D1 and PARP1 was examined in MCF7 cells (left) or MCF7 cells that were transfected with FLAG-NR1D1 (right) after 0.5 μmol/L doxorubicin (Doxo) treatment for 4 hours. Whole cell lysates were immunoprecipitated (IP) and probed by Western blotting (WB). **B,** MCF7 cells were subjected to *in situ* PLA. As a negative control, a single staining with the anti-NR1D1 or anti-PARP1 antibody was performed. Nuclei were stained by DAPI (gray). **C,** PARylation of NR1D1 was determined in the MCF7 cells that were transfected with Myc-NR1D1 after 0.5 μmol/L doxorubicin (Doxo) treatment for 4 hours. Whole cell lysates were immunoprecipitated and probed by Western blotting. **D,** *In vitro* PARylation assay was performed using the recombinant GST-PARP1 (rPARP1) and GST-NR1D1-His (rNR1D1) proteins. The reaction mixtures were stained with Coomassie (left) and immunoblotted using anti-PAR antibody (right). **E,** Lack of PARylation in the hinge deletion mutant (ΔHinge) or the LBD deletion mutant (ΔLBD) of NR1D1. PARylation was determined as described in **C**. **F,** NHEJ or HR efficiency was determined in MCF7 cells that were cotransfected with the indicated constructs. *, $P < 0.05$ and not significant (ns) versus empty vector (EV); $^{\#}$, $P < 0.05$ versus NR1D1 Full ($n = 4$). Expression level of NR1D1 is shown as control in Supplementary Fig. S1D.

NR1D1 is recruited to DSB sites and then suppresses further recruitment of DDR complex

Because many DNA repair factors are PARylated to access DNA damage sites, we examined the possibility that PARylated NR1D1 is recruited to DNA breakage sites. Surprisingly, laser microirradiation analysis showed that NR1D1 was recruited rapidly to the irradiated sites, whereas PHEN, a PARP inhibitor, dramatically decreased the recruitment of NR1D1. Also the ΔLBD was defective to access the damaged DNA, suggesting that binding to PARP1 and subsequent PARylation is essential for the recruitment of NR1D1 (Fig. 3A and Supplementary Fig. S4). The wild-type FokI, but not the D450A mutant, generated single DSB site in chromosome, which was overlaid with NR1D1, further demonstrating the association of NR1D1 in DNA breakage sites (Fig. 3B). Interestingly, NR1D1 formed nuclear foci following doxorubicin treatment, which were overlaid with γH2AX foci. In the presence of PHEN, the number of overlaid γH2AX/NR1D1 foci decreased mainly due to the disappearance of NR1D1 foci (Fig. 3C). Next, we analyzed the recruitment of NR1D1 to the DSB sites generated by exogenously introduced I-*Sce*I on the NHEJ or HR reporter plasmid. ChIP analysis showed that NR1D1 was recruited to the DSB sites on both reporters at 24 h after I-*Sce*I transfection (Fig. 3D and Supplementary Fig. S1E). Recruitment of the DDR factors such as γH2AX, PARP1, SIRT6, pNBS1, and BRCA1 were peaked at 24 h after I-*Sce*I transfection in control cells. However, the recruitment peaks were delayed to 36 hours in the presence of NR1D1 (Fig. 3E and Supplementary Fig. S1E and Supplementary Fig. S5). Taken together, these results show that NR1D1 is recruited to DNA damage sites in a PARP1-dependent manner and inhibits further recruitment of other DDR factors.

NR1D1 increases the sensitivity of breast cancer cells to doxorubicin

DNA repair deficiency in cancer cells sensitizes them to DNA damaging agents, so we determined whether NR1D1 makes cells sensitive to doxorubicin. First, we established two stable MCF7 sublines, in which NR1D1 expression was suppressed (Supplementary Fig. S6A). First, we examined the formation of γH2AX foci in the shGFP control and shNR1D1-MCF7 cells. Doxorubicin treatment increased the number of γH2AX foci in both cell lines,

however, it decreased more rapidly in the shNR1D1-MCF7 than shGFP control cells, supporting that NR1D1 delays the DDR (Fig. 4A and Supplementary Fig. S6B). In agreement, the shNR1D1-MCF7 cells were less sensitive to doxorubicin-induced inhibition of cell survival in diverse culture systems compared with control (Fig. 4B and C and Supplementary Fig. S6C and

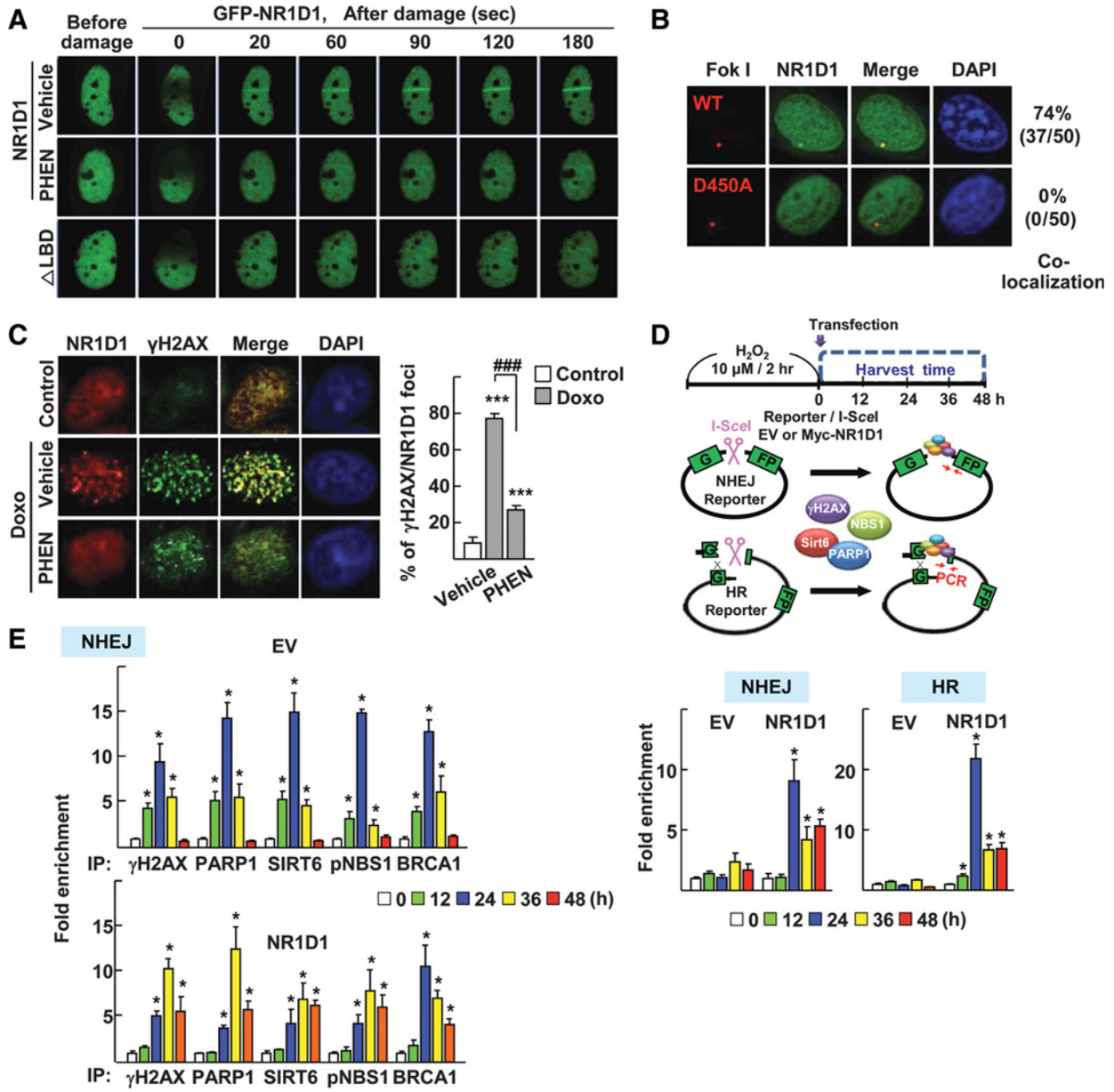

Figure 3.

PARylation of NR1D1 is required for its recruitment to DSB sites. **A,** Laser microirradiation experiments were performed with MCF7 cells transfected with GFP-fused NR1D1 or LBD deletion mutant (ΔLBD) in the presence or absence of 100 μmol/L PHEN. Quantification of mean fluorescence intensity at the microirradiated site is presented in Supplementary Fig. S4. **B,** U2OS-DSB reporter cells were cotransfected with mCherry-LacI-FokI wild-type (WT) or nuclease-deficient mCherry-LacI-FokI (D450A) and GFP-NR1D1. After 48 h, cells were fixed and analyzed using confocal microscopy. The number of cells in which NR1D1 (green) was colocalized with FokI (red) was counted and is presented as percentage of 50 FokI-positive cells. **C,** MCF7 cells were treated with 1 μmol/L doxorubicin (Doxo) for 1 h in the presence or absence of 100 μmol/L PHEN. Cells were fixed and immunostained with anti-NR1D1 (red) and anti-γH2AX antibody (green; left). The number of γH2AX-positive foci that were also NR1D1-positive was quantified and is presented as percentage of the number of total γH2AX-positive foci from 50 cells (right). ***, $P < 0.001$ versus no treatment (control) and ###, $P < 0.001$ versus doxorubicin with vehicle ($n = 3$). **D,** Schematic representation of ChIP assays (top). MCF7 cells were treated with 10 μmol/L H_2O_2 for 2 hours and then transfected with NHEJ or HR reporter plasmid, I-*Sce*I expressing vector, and empty vector (EV) or Myc-NR1D1. Cells were fixed at the indicated time and subjected to ChIP assays using anti-Myc. *, $P < 0.05$ versus 0 hour ($n = 3$; bottom). **E,** The same cell lysates of **D** were subjected to ChIP assays using specific antibodies as indicated. *, $P < 0.05$ versus 0 hour ($n = 3$). Expression level of NR1D1 for **D** and **E** is shown as control in Supplementary Fig. S1E.

S6D). Importantly, GSK4112 increased the sensitivity of cells to doxorubicin-induced suppression of cell survival (Supplementary Fig. S6E and S6F). This sensitizing effect of GSK4112 was also supported by clonal growth inhibition in control cells, but not in the shNR1D1-MCF7 cells (Fig. 4D and Supplementary Fig. S6G). Next, we examined the *in vivo* susceptibility to doxorubicin in these stable cells based on xenograft experiments. Tumor growth in control MCF7 cells was significantly inhibited by doxorubicin treatment, whereas that in shNR1D1-MCF7 cells was not affected (Fig. 4E). Immunohistochemical analyses of the tumor tissues showed that γH2AX levels increased greatly in the doxorubicin-treated shGFP control group, but less in the shNR1D1-MCF7 group (Fig. 4F and Supplementary Fig. S7). The binding of NR1D1 with PARP1 was clearly observed in the specimens from the xenografted shGFP-MCF7 cells that were treated with doxorubicin when examined by PLA assay (Fig. 4G).

High NR1D1 expression is associated with better clinical outcomes in breast cancer patients

Given that NR1D1 modulates the chemosensitivity of breast cancer cells in both *in vitro* and *in vivo* experiments, we asked whether intratumoral NR1D1 expression is associated with response to chemotherapy in breast cancer patients. We analyzed the gene expression profiles obtained from public datasets, which included clinical outcome information such as pathologic complete response (pCR), disease-free survival (DFS), and relapse-free survival (RFS). The pCR is an important marker of improved chemosensitivity in solid tumors, which correlates with a favorable DFS and overall survival (32). In two independent datasets, GSE4056 and GSE34138, the subgroups of patients with high NR1D1 expression levels had higher pCR rates (26, 27). The odds ratio, which describes the impact of predictor variables (33), was 3.75 for GSE4056 and 2.11 for GSE34138, thus the results indicate a positive correlation between the NR1D1 expression level and a better clinical outcome in breast cancer patients (Table 1). In agreement with this finding, the NR1D1 expression level was higher in the patients of the achieved pCR group than in the patients from the nonachieved pCR group, with statistical or marginal significance in these datasets (Supplementary Fig. S8). In addition, we analyzed the survival rates using the Kaplan–Meier method with the log-rank test in two independent datasets, GSE1456 and NKI (28, 29). RFS or DFS was improved in the high NR1D1 expression group, which indicates a beneficial effect of chemotherapy on recurrence in patients with high NR1D1 expression levels (Fig. 5A). Finally, we demonstrated the colocalization of NR1D1 with γH2AX foci and the specific interaction of NR1D1 with PARP1 in human breast cancer specimens, which is probably associated with the sensitivity of breast cancer cells to chemotherapy (Fig. 5B and 5C).

Discussion

In this study, we demonstrated for the first time that NR1D1 inhibits recruitment of the DDR complex to damaged DNA sites, thereby impairing proper DNA repair. Interestingly, we found that NR1D1 is PARylated by physical interaction with PARP1 and the PARylation is required for recruitment of NR1D1 to damaged DNA sites. In agreement, NR1D1 increased the sensitivity of breast cancer cells to doxorubicin in both *in vitro* and *in vivo* experiments. A plausible mechanism for the action of NR1D1 could involve its recruitment by PARP1 to hinder the recruitment of DDR factors to DNA damage sites. Intriguingly, however, PARP inhibitors have been examined as sensitizing agents to chemotherapy and radiotherapy (34). Several PARP inhibitors including Olaparib, Veliparib, and Rucaparib are in phases II and III clinical trials as monotherapy or combination therapies (35). Nevertheless, only about 40% of BRCA-deficient breast and ovarian cancers respond to PARP inhibitors, suggesting that PARP1 may function beyond a simple direction of DNA repair (36, 37). Temporal and spatial evaluations of PARylation of DDR components including NR1D1 could yield more precise understanding of the regulation of DDR, which could provide better strategies for breast cancer treatment.

This study has identified NR1D1 as a negative regulator of DNA repair, which increases sensitivity to chemotherapeutic agents. However, it is widely recognized that defects in DNA repair system lead to genomic instability, which is one of the most prevalent characteristics of cancer (38). Thus, although NR1D1 could provide therapeutic opportunities, it may cause genomic instability and ultimately drive mammary tumorigenesis. Indeed, *NR1D1* gene is encoded within the *ERBB2* amplicon and the expression level of this receptor is correlated with a poor prognosis (12, 13). Further, NR1D1 enhances the survival of breast cancer cells, suggesting a potential role for NR1D1 in breast cancer development (14). A better understanding of the NR1D1-induced cellular response to DNA damage and repair at different steps of mammary tumorigenesis may provide benefits for developing strategies for prognosis and treatment of the disease.

Chemotherapy has contributed greatly to reduce mortality in patients with cancer, but it also decreases the quality of life due to severe side effects. Therefore, novel therapeutic options are required to reduce the dosages in chemotherapy to avoid unwanted toxicity. In particular, the DNA repair machinery has been considered as a target for establishing novel therapeutic options. Inhibitors of DNA repair components such as ATM, ATR, DNA-PK, Chk1, and Chk2 have been developed as chemosensitizers in clinical trials (39). Here, we report that NR1D1 expression was negatively correlated with the DNA repair efficiency in breast cancer cell lines and that the NR1D1 agonist, GSK4112, sensitized breast cancer cells to doxorubicin (Fig. 1B and 4D). Thus, these findings may provide a potential chemosensitizer to enhance the outcomes of adjuvant chemotherapy. Interestingly, several other nuclear receptors have been reported to regulate the DNA damage repair machinery. NR4A is recruited to ionizing radiation- or ultraviolet-induced DNA damage sites and it promotes DNA repair (40, 41). Thyroid hormone receptor β induces cellular senescence and DNA damage in mouse embryonic fibroblasts and hepatocytes, while testicular nuclear receptor 4 regulates ATM expression and functions as a tumor suppressor in prostate cancer (42, 43). Recently, Izhar and colleagues (44) reported that nine nuclear receptors, including ESRRA and RARB, were localized to the sites of DNA damage after laser microirradiation. These observations together with our results suggest that nuclear receptor ligands could provide better therapies when combined with current chemotherapeutic agents. Further investigations of the relationships between the expression levels of these receptors and the clinical outcomes of chemotherapy in breast cancer patients may expand the spectrum of therapeutic options.

NR1D1 is a well-known component of the circadian clock, which regulates the expression of circadian clock genes such as BMAL1 and CLOCK (11). Increasing evidence indicates that the efficiency of DNA repair oscillates with the circadian rhythm and the circadian clock system is closely linked to the sensitivity of chemotherapy (45). Recently, several attempts have been made to

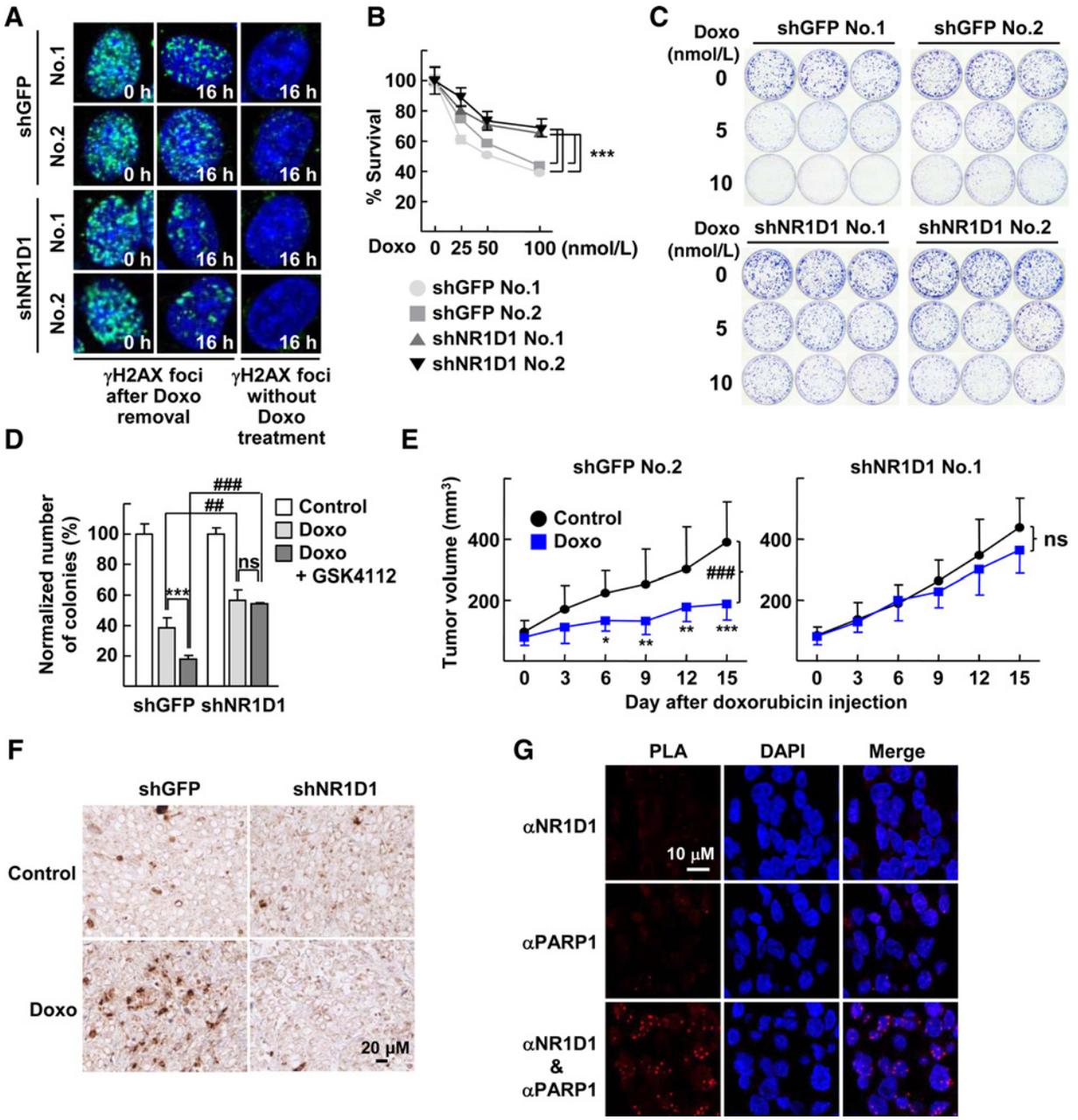

Figure 4.

Lack of NR1D1 decreases sensitivity to doxorubicin. **A,** Clearance of γH2AX was monitored in the MCF7 stable cell lines that expressed shGFP or shNR1D1 after 1 μmol/L doxorubicin (Doxo) treatment for 1 hour. Cells were fixed at 16 hours after removal of doxorubicin and were immunostained with anti-γH2AX antibody (green). Quantification of γH2AX foci is presented in Supplementary Fig. S6B. **B,** The MCF7 stable cells were exposed to doxorubicin for 72 hours. Relative cell viability was analyzed using MTT assay. ***, $P < 0.001$ ($n = 3$). **C,** The MCF7 stable cells were exposed to doxorubicin for 14 days, and clonogenic survival assays were performed. Images are representative of those obtained from three independent experiments. Quantification of the number of colonies is presented in Supplementary Fig. S6C. **D,** The MCF7 stable cells were exposed to 5 nmol/L doxorubicin and/or 5 μmol/L GSK4112 for 14 days. Colonies that were composed of more than 50 cells were counted. ***, $P < 0.001$; ##, $P < 0.01$; and ###, $P < 0.001$ ($n = 3$). Representative images are shown in Supplementary Fig. S6G. **E,** Female athymic nude mice were injected subcutaneously with the MCF7 stable cells. When tumors were approximately 100 mm^3, mice were given intraperitoneal injections with doxorubicin at a dose of 4 mg/kg at 4 days interval, with a total of three injections. Tumor volume was measured with a caliper. The number of specimen of each group was as follows: shGFP-control ($n = 14$), shGFP-doxorubicin ($n = 12$), shNR1D1-control ($n = 8$), and shNR1D1-doxorubicin ($n = 8$). *, $P < 0.05$; **, $P < 0.01$; ***, $P < 0.001$ versus control at the indicated time; ###, $P < 0.001$ versus control. **F,** Representative images of immunohistochemistry staining for γH2AX in tumor sections. Images from several tumor samples and the quantification of staining intensity are presented in Supplementary Fig. S7. **G,** PLA was performed in tumor sections with anti-NR1D1 and anti-PARP1 antibodies. As a negative control, a single staining with the anti-NR1D1 or anti-PARP1 is shown. Nuclei were stained by DAPI.

Table 1. Increased therapeutic response in breast cancer patients with high NR1D1 expression[a]

Data set	NR1D1 expression[b]	Non-pCR	pCR	*P*-value	Odd ratio of pCR[c] (95% CI)
GSE4056 (test set)	low	20 (90.9%)	2 (9.1%)	0.2404	3.75 (0.6647–21.1546)
	high	16 (72.7%)	6 (27.3%)		
GSE34138	low	67 (75.3%)	22 (24.7%)	0.0254	2.1084 (1.1092–4.0077)
	high	52 (59.1%)	36 (40.9%)		

Abbreviation: CI, confidence interval.

[a]The GSE4056 and GSE34138 datasets that have therapeutic response information were obtained from NCBI GEO site.

[b]Patients were categorized into a low (below median) NR1D1 expression group and a high (above median) NR1D1 expression group. The expression levels of NR1D1 in an individual patient in each NR1D1 low and high group and their median values are shown in Supplementary Fig. S8.

[c]The Fisher exact probability test was performed for determination of significance by a web-based program (http://vassarstats.net/).

develop chronochemotherapy, a circadian-based anticancer approach for determining the optimal circadian time to achieve the best therapeutic index (46). According to a recent meta-analysis, chronotherapy with oxaliplatin, 5-fluorouracil, and leucovorin improved overall survival in men with metastatic colorectal cancer compared with conventional chemotherapy (47). Our demonstration that the efficacy of DSB repair was modulated by NR1D1 in breast cancer cells strongly supports the potential benefits of chronotherapy based on the oscillation of NR1D1 expression.

Recently, many studies have aimed to identify useful markers to determine the outcomes of chemotherapy. In the present study, we found that breast cancer patients with high NR1D1 expression levels had better clinical outcomes after chemotherapy in clinics (Table 1 and Fig. 5A). This observation may indicate that NR1D1 increases the sensitivity of breast cancer cells to DNA damage-inducing chemotherapy, thereby facilitating the successful achievement of pCR in breast cancer patients. The achievement of pCR with primary chemotherapy is crucial for the successful treatment of patients with breast cancer, so careful consideration is required to identify the best therapeutic option. We suggest that NR1D1 could be used as a novel predictive biomarker for breast cancer to facilitate a more personalized treatment approach. Interestingly, most of the cell lines that we tested contain mutations in *p53* and/or allelic loss of *BRCA1*, which suggests that the loss of DNA repair capacity may facilitate NR1D1-induced DNA repair impairment (48, 49). Therefore, further detailed analyses of the NR1D1 gene expression level and alterations in genes involved with the DDR response may improve the prediction of outcomes with DNA damage-inducing chemotherapy. In particular, patients with TNBC frequently possess germline *BRCA1* mutations and various phenotypic characteristics in BRCA1-related breast cancer, including silencing of *BRCA1* or mutations in other DNA repair-related genes such as *p53* (50). Therefore, TNBC

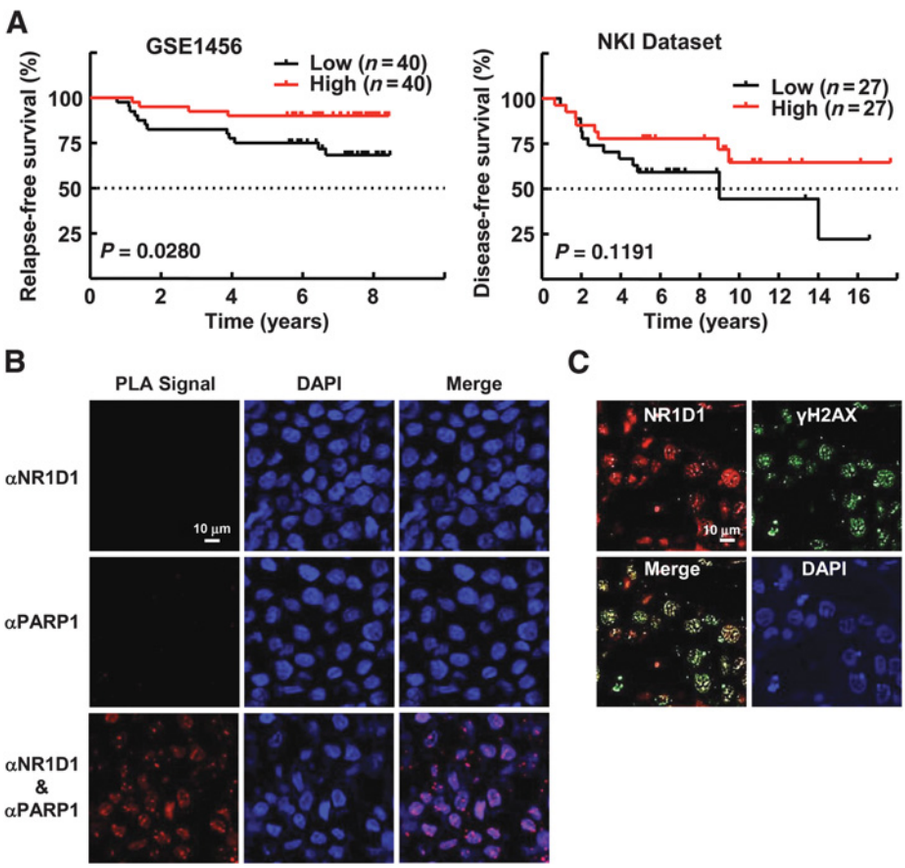

Figure 5.
High Nr1d1 expression is correlated with an improved clinical outcome in breast cancer patients received chemotherapy. **A,** The GSE1456 and the NKI data sets were obtained from NCBI GEO site and a web site provided by Dr. Bernards and his colleagues, respectively. Patients were categorized into a low NR1D1 expression (lower quartile) group and a high NR1D1 expression (upper quartile) group. DFS or RFS rate (%) was plotted for each group. To analyze statistical differences, Log-rank (Mantel–Cox) tests were performed. **B,** PLA was performed in breast cancer specimens with anti-NR1D1 and anti-PARP1 antibodies. As a negative control, a single staining with the anti-NR1D1 or anti-PARP1 was performed. **C,** Colocalization of NR1D1 and γH2AX. Breast cancer specimens were immunostained with anti-NR1D1 (red) and anti-γH2AX (green).

could be a primary target for testing our hypothetical use of NR1D1 as a predictive biomarker for breast cancer chemotherapy to facilitate a more personalized treatment approach in the future.

Disclosure of Potential Conflicts of Interest

No potential conflicts of interest were disclosed.

Authors' Contributions

Conception and design: N.-L. Ka, T.-Y. Na, M.-O. Lee
Development of methodology: N.-L. Ka, M.-O. Lee
Acquisition of data (provided animals, acquired and managed patients, provided facilities, etc.): N.-L. Ka, T.-Y. Na, H. Na, M.-H. Lee, H.-S. Park, S. Hwang, I.Y. Kim
Analysis and interpretation of data (e.g., statistical analysis, biostatistics, computational analysis): N.-L. Ka, H. Na, I.Y. Kim, J.K. Seong, M.-O. Lee
Writing, review, and/or revision of the manuscript: N.-L. Ka, M.-O. Lee
Administrative, technical, or material support (i.e., reporting or organizing data, constructing databases): S. Hwang
Study supervision: J.K. Seong, M.-O. Lee

Grant Support

This work was supported by grants, the NRF-2014R1A2A1A10052265 to M.-O. Lee, the NRF-2014M3A9D5A01073556 to M.-O. Lee and J.K. Seong, and the NRF-2013H1A2A1033512 to N.-L. Ka from the National Research Foundation of Korea and a grant (1220110 to M.-O. Lee) from the National R&D Program for Cancer Control, Ministry of Health & Welfare, Korea.

The costs of publication of this article were defrayed in part by the payment of page charges. This article must therefore be hereby marked *advertisement* in accordance with 18 U.S.C. Section 1734 solely to indicate this fact.

Received August 5, 2016; revised September 12, 2016; accepted February 16, 2017; published OnlineFirst March 1, 2017.

References

1. Ferlay J, Soerjomataram I, Dikshit R, Eser S, Mathers C, Rebelo M, et al. Cancer incidence and mortality worldwide: sources, methods and major patterns in GLOBOCAN 2012. Int J Cancer 2015;136:E359–86.
2. Senkus E, Kyriakides S, Ohno S, Penault-Llorca F, Poortmans P, Rutgers E, et al. Primary breast cancer: ESMO Clinical Practice Guidelines for diagnosis, treatment and follow-up. Ann Oncol 2015;26:v8–30.
3. Hernandez-Aya LF, Gonzalez-Angulo AM. Adjuvant systemic therapies in breast cancer. Surg Clin North Am 2013;93:473–91.
4. Liedtke C, Rody A. New treatment strategies for patients with triple-negative breast cancer. Curr Opin Obstet Gynecol 2015;27:77–84.
5. Goldstein M, Kastan MB. The DNA damage response: implications for tumor responses to radiation and chemotherapy. Annu Rev Med 2015; 66:129–43.
6. Lord CJ, Ashworth A. The DNA damage response and cancer therapy. Nature 2012;481:287–94.
7. Curtin NJ.DNA repair dysregulation from cancer driver to therapeutic target. Nat Rev Cancer 2012;12:801–17.
8. Bouwman P, Jonkers J. The effects of deregulated DNA damage signalling on cancer chemotherapy response and resistance. Nat Rev Cancer 2012; 12:587–98.
9. Chen Y, Kamili A, Hardy JR, Groblewski GE, Khanna KK, Byrne JA. Tumor protein D52 represents a negative regulator of ATM protein levels. Cell Cycle 2013;12:3083–97.
10. Li W, Katoh H, Wang L, Yu X, Du Z, Yan X, et al. FOXP3 regulates sensitivity of cancer cells to irradiation by transcriptional repression of BRCA1. Cancer Res 2013;73:2170–80.
11. Everett LJ, Lazar MA. Nuclear receptor Rev-erbα: up, down, and all around. Trends Endocrinol Metab 2014;25:586–92.
12. Chin K, DeVries S, Fridlyand J, Spellman PT, Roydasgupta R, Kuo WL, et al. Genomic and transcriptional aberrations linked to breast cancer pathophysiologies. Cancer Cell 2006;10:529–41.
13. Davis LM, Harris C, Tang L, Doherty P, Hraber P, Sakai Y, et al. Amplification patterns of three genomic regions predict distant recurrence in breast carcinoma. J Mol Diagn 2007;9:327–36.
14. Kourtidis A, Jain R, Carkner RD, Eifert C, Brosnan MJ, Conklin DS. An RNA interference screen identifies metabolic regulators NR1D1 and PBP as novel survival factors for breast cancer cells with the ERBB2 signature. Cancer Res 2010;70:1783–92.
15. Muscat GE, Eriksson NA, Byth K, Loi S, Graham D, Jindal S, et al. Research resource: nuclear receptors as transcriptome: discriminant and prognostic value in breast cancer. Mol Endocrinol 2013;27:350–65.
16. Wang Y, Kojetin D, Burris TP. Anti-proliferative actions of a synthetic REV-ERBα/β agonist in breast cancer cells. Biochem Pharmacol 2015; 96:315–22.
17. Burris TP.Nuclear hormone receptors for heme: REV-ERBalpha and REV-ERBbeta are ligand-regulated components of the mammalian clock. Mol Endocrinol 2008;22:1509–20.
18. Mao Z, Hine C, Tian X, Van Meter M, Au M, Vaidya A, et al. SIRT6 promotes DNA repair under stress by activating PARP1. Science 2011;332:1443–46.
19. Shanbhag NM, Rafalska-Metcalf IU, Balane-Bolivar C, Janicki SM, Greenberg RA. ATM-dependent chromatin changes silence transcription in cis to DNA double-strand breaks. Cell 2010;141:970–81.
20. Min S, Jo S, Lee HS, Chae S, Lee JS, Ji JH, et al. ATM-dependent chromatin remodeler Rsf-1 facilitates DNA damage checkpoints and homologous recombination repair. Cell Cycle 2014;13:666–77.
21. Soo Lee N, Jin Chung H, Kim HJ, Yun Lee S, Ji JH, Seo Y, et al. et al.TRAIP/RNF206 is required for recruitment of RAP80 to sites of DNA damage. Nat Commun 2016;7:10463.
22. Kang HJ, Lee MH, Kang HL, Kim SH, Ahn JR, Na H, et al. Differential regulation of estrogen receptor alpha expression in breast cancer cells by metastasis-associated protein 1. Cancer Res 2014;74:1484–94.
23. Seluanov A, Mittelman D, Pereira-Smith OM, Wilson JH, Gorbunova V. DNA end joining becomes less efficient and more error-prone during cellular senescence. Proc Natl Acad Sci U S A 2004;101:7624–29.
24. Na TY, Ka NL, Rhee H, Kyeong D, Kim MH, Seong JK, et al. Interaction of Hepatitis B Virus X Protein with PARP1 results in inhibition of DNA repair in hepatocellular carcinoma. Oncogene 2016;35:5435–5445.
25. Han YH, Kim DK, Na TY, Ka NL, Choi HS, Lee MO. RORalpha switches transcriptional mode of ERRgamma that results in transcriptional repression of CYP2E1 under ethanol-exposure. Nucleic Acids Res 2015; 44:1095–104.
26. Thuerigen O, Schneeweiss A, Toedt G, Warnat P, Hahn M, Kramer H, et al. Gene expression signature predicting pathologic complete response with gemcitabine, epirubicin, and docetaxel in primary breast cancer. J Clin Oncol 2006;24:1839–45.
27. de Ronde JJ, Lips EH, Mulder L, Vincent AD, Wesseling J, Nieuwland M, et al. SERPINA6, BEX1, AGTR1, SLC26A3, and LAPTM4B are markers of resistance to neoadjuvant chemotherapy in HER2-negative breast cancer. Breast Cancer Res Treat 2013;137:213–23.
28. Pawitan Y, Bjöhle J, Amler L, Borg AL, Egyhazi S, Hall P, et al. Gene expression profiling spares early breast cancer patients from adjuvant therapy: derived and validated in two population-based cohorts. Breast Cancer Res 2005;7:R953–64.
29. van de Vijver MJ, He YD, van't Veer LJ, Dai H, Hart AA, Voskuil DW, et al. A gene-expression signature as a predictor of survival in breast cancer. N Engl J Med. 2002;347:1999–2009.
30. Yang F, Teves SS, Kemp CJ, Henikoff S. Doxorubicin, DNA torsion, and chromatin dynamics. Biochim Biophys Acta 2014;1845:84–9.
31. Sousa FG, Matuo R, Soares DG, Escargueil AE, Henriques JA, Larsen AK, et al. PARPs and the DNA damage response. Carcinogenesis 2012;33: 1433–40.
32. Cortazar P, Zhang L, Untch M, Mehta K, Costantino JP, Wolmark N, et al. Pathological complete response and long-term clinical benefit in breast cancer: the CTNeoBC pooled analysis. The Lancet 2014;384:164–72.
33. Szumilas M.Explaining odds ratios. J Can Acad Child Adolesc Psychiatry 2010;19:227–9.
34. Tangutoori S, Baldwin P, Sridhar S. PARP inhibitors: A new era of targeted therapy. Maturitas 2015;81:5–9.

35. Livraghi LGarber JE PARP inhibitors in the management of breast cancer: current data and future prospects. BMC Med 2015;13:188.
36. Tutt A, Robson M, Garber JE, Domchek SM, Audeh MW, Weitzel JN, et al. Oral poly(ADP-ribose) polymerase inhibitor olaparib in patients with BRCA1 or BRCA2 mutations and advanced breast cancer: a proof-of-concept trial. Lancet 2010;376:235–44.
37. Audeh MW, Carmichael J, Penson RT, Friedlander M, Powell B, Bell-McGuinn KM, et al. Oral poly(ADP-ribose) polymerase inhibitor olaparib in patients with BRCA1 or BRCA2 mutations and recurrent ovarian cancer: a proof-of-concept trial. Lancet 2010;376:245–51.
38. Venkatesan S, Natarajan AT, Hande MP. Chromosomal instability–mechanisms and consequences. Mutat Res Genet Toxicol Environ Mutagen 2015;793:176–84.
39. Furgason JM, Bahassi el M. Targeting DNA repair mechanisms in cancer. Pharmacol Ther 2013;137:298–308.
40. Malewicz M, Kadkhodaei B, Kee N, Volakakis N, Hellman U, Viktorsson K, et al. Essential role for DNA-PK-mediated phosphorylation of NR4A nuclear orphan receptors in DNA double-strand break repair. Genes Dev 2011;25:2031–40.
41. Jagirdar K, Yin K, Harrison M, Lim W, Muscat GE, Sturm RA, et al. The NR4A2 nuclear receptor is recruited to novel nuclear foci in response to UV irradiation and participates in nucleotide excision repair. PLoS One 2013;8:e78075.
42. Zambrano A, García-Carpizo V, Gallardo ME, Villamuera R, Gómez-Ferrería MA, Pascual A, et al. The thyroid hormone receptor beta induces DNA damage and premature senescence. J Cell Biol 2014;204:129–46.
43. Lin SJ, Lee SO, Lee YF, Miyamoto H, Yang DR, Li G, et al. TR4 nuclear receptor functions as a tumor suppressor for prostate tumorigenesis via modulation of DNA damage/repair system. Carcinogenesis 2014;35:1399–1406.
44. Izhar L, Adamson B, Ciccia A, Lewis J, Pontano-Vaites L, Leng Y, et al. A systematic analysis of factors localized to damaged chromatin reveals PARP-dependent recruitment of transcription factors. Cell Rep 2015;11:1486–1500.
45. Sancar A, Lindsey-Boltz LA, Gaddameedhi S, Selby CP, Ye R, Chiou YY, et al. Circadian clock, cancer, and chemotherapy. Biochemistry 2015;54:110–23.
46. Innominato PF, Roche VP, Palesh OG, Ulusakarya A, Spiegel D, Lévi FA. The circadian timing system in clinical oncology. Ann Med 2014;46:191–207.
47. Giacchetti S, Dugué PA, Innominato PF, Bjarnason GA, Focan C, Garufi C, et al. Sex moderates circadian chemotherapy effects on survival of patients with metastatic colorectal cancer: a meta-analysis. Ann Oncol 2012;23:3110–16.
48. Elstrodt F, Hollestelle A, Nagel JH, Gorin M, Wasielewski M, van den Ouweland A, et al. BRCA1 mutation analysis of 41 human breast cancer cell lines reveals three new deleterious mutants. Cancer Res 2006;66:41–5.
49. Hollestelle A, Nagel JH, Smid M, Lam S, Elstrodt F, Wasielewski M, et al. Distinct gene mutation profiles among luminal-type and basal-type breast cancer cell lines. Breast Cancer Res Treat 2010;121:53–64.
50. Cancer Genome Atlas Network. Comprehensive molecular portraits of human breast tumours. Nature 2012;490:61–70.